



Josephson current and multiple Andreev reflections in graphene SNS junctions

Xu Du, Ivan Skachko, and Eva Y. Andrei

Department of Physics and Astronomy, Rutgers University, Piscataway, New Jersey 08854, USA

(Received 26 March 2008; published 9 May 2008)

The Josephson effect and superconducting proximity effect were observed in superconductor-graphene-superconductor (SGS) Josephson junctions with coherence lengths comparable to the distance between the superconducting leads. By comparing the measured gate dependence of the proximity induced subgap features (multiple Andreev reflections) and of the supercurrent to theoretical predictions, we find that the diffusive junction model yields close quantitative agreement with the results. By contrast, predictions of the ballistic SGS model are inconsistent with the data. We show that all SGS devices reported so far, our own as well as those of other groups, fall in the diffusive junction category. This is attributed to substrate induced potential fluctuations due to trapped charges and to the invasiveness of the metallic leads.

DOI: [10.1103/PhysRevB.77.184507](https://doi.org/10.1103/PhysRevB.77.184507)

PACS number(s): 74.45.+c, 73.50.Gr, 73.63.-b, 81.05.Uw

INTRODUCTION

The discovery of methods to extract single atomic layers from graphite^{1,2} (graphene) has triggered a torrential effort to explore the new physical properties emerging from their relativistic (Dirac) quasiparticle spectrum.²⁻⁴ A particularly interesting set of questions and expectations has arisen with the recent fabrication of graphene-superconductor (GS) hybrid structures,^{5,6} which has made it feasible to study the interplay between superconductivity and relativistic quantum dynamics. Because of the chemical inertness of graphene, achieving transparent interfaces is relatively easy and reproducible compared to other gate controllable junctions where the weak link is a semiconductor or a two-dimensional electron gas.^{7,8} With almost ideal interfaces, and the ability to carry bipolar supercurrents that are gate tunable from electron to the hole branch,^{5,9} the superconductor-graphene-superconductor (SGS) junctions are promising candidates for nanoelectronics applications as well as for studying the physics and “phase diagram” of Josephson junctions.¹⁰ It is therefore important to understand the basic properties of experimentally realizable SGS junctions. These properties are expected to be controlled by the transport of relativistic electrons across the GS interface, which is qualitatively different from the transport of normal electrons. Whereas a normal electron impinging on a normal-superconductor (NS) interface is “retroreflected” as a hole (Andreev reflection) retracing the same trajectory,¹¹⁻¹³ the process is specular for relativistic electrons¹⁴ (if the Fermi energy is within the superconducting gap). These “specular Andreev reflections” (SARs) are expected to clearly leave manifest marks in ballistic SGS junctions, where the electron mean free path exceeds the junction length, detectable through a strong and unusual gate dependence of the multiple Andreev reflections (MARs).^{11-13,15} Furthermore, in ballistic SGS junctions, the Josephson critical current I_c and the product $I_c R_n$ (R_n is the normal state resistance) are expected to exhibit a characteristic gate dependence, which is qualitatively different from that of conventional SNS junctions.^{9,16}

Many proposed physical phenomena and devices based on SGS junctions implicitly assume ballistic transport because, due to the unique properties such as chirality and

Zitterbewegung,^{17,18} the carriers in graphene are expected to have low scattering rates and long mean free paths (MFPs). Surprisingly, thus far, there is no solid experimental evidence in support of ballistic transport or of relativistic charge carriers in SGS. Here, we show that SGS junctions fabricated on Si/SiO₂ substrates with present day techniques are, in fact, diffusive with MFP much shorter than the junction length. In these junctions, we find close quantitative agreement between predictions of the diffusive SNS junction model and all aspects of the data, including the gate dependence of the MAR, the I_c , and of the product $I_c R_n$. By contrast, predictions of the ballistic SGS junction model are shown to be inconsistent with the experimental results.

EXPERIMENTAL SETUP

SGS junctions were fabricated with mechanically exfoliated single layer graphene¹ deposited onto Si($p+$)/SiO₂(300 nm) substrates that were prepatterned with alignment marks. Following the identification of graphene with a combination of optical imaging and atomic force microscopy (AFM), the leads, Al(30 nm)/Ti(2 nm), were fabricated using standard e-beam lithography and lift-off. Distances between the leads were in the range $L \sim 200$ – 400 nm and the aspect ratios $W/L \sim 10$ – 30 , where W is the junction width. An optical image of a typical device is shown in the upper inset of Fig. 1(a). Measurements were carried out in a dilution refrigerator with the base temperature of 100 mK using a standard four-lead technique. Back-gate voltage, V_g , applied to the Si substrate was used to control the carrier density in graphene $n \sim 7.4 \times 10^{10} |V_g| \text{cm}^{-2}$. Two stage RC filters at low temperature (4 K) and a bank of pi filters at room temperature were used for noise filtering.

RESULTS AND ANALYSIS

Upon cooling far below the critical temperature of the leads, $T_c \sim 1$ K, the current voltage characteristics (IVC) show sharp switching between Josephson and normal currents, as illustrated in Fig. 1(a). For convenience, unless specified otherwise, we will show detailed data only from sample S032007, with length $L=350$ nm and width W

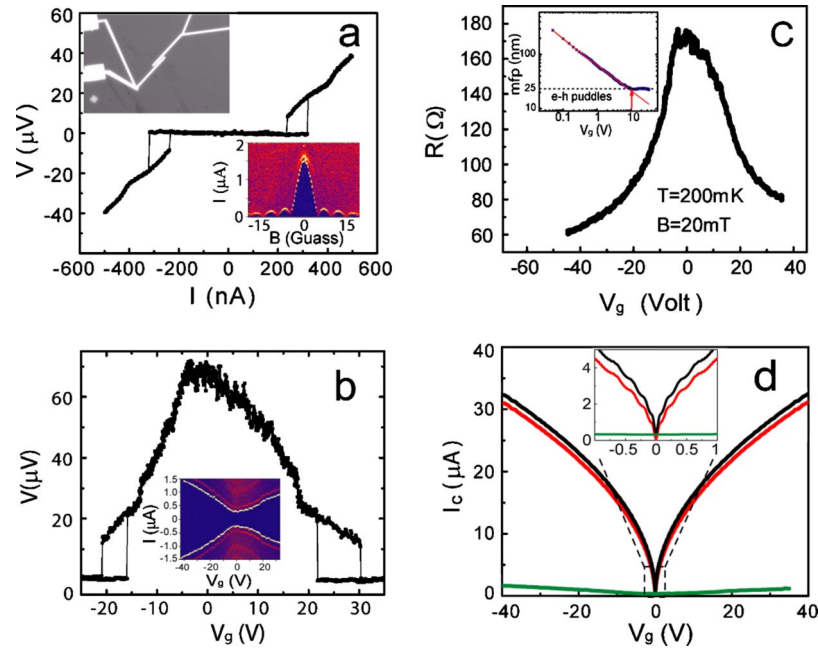


FIG. 1. (Color online) (a) Main panel: IVC showing Josephson state at $T=200$ mK. Upper inset: optical image of a device. Lower inset: magnetic field dependence of critical current exhibiting Fraunhofer pattern. (b) Gate dependence of the voltage across a junction in Josephson state for $I=800$ nA. Inset: IV curves as a function of gate voltage. The center area corresponding to the Josephson state is separated from the normal state by the switching current represented by the bright line. (c) Gate dependence of normal state resistance at $T=200$ mK. The superconductivity of the leads was suppressed with a small magnetic field. Inset: mean free path calculated from the transport data. The arrow indicates the onset of the puddle regime. (d) Gate dependence of critical current. Comparison of the data with theoretical predictions for ballistic SGS junction at $T=0$. Green line (dark gray) represents the experimental data; solid black line is the calculated value without fluctuation, and the red (light gray) is the calculated value with fluctuations due to a rf noise temperature of 300 mK. Inset: zoom into Dirac point.

$=9 \mu\text{m}$. Most data shown here pertain to this sample, but the other samples (five samples were measured) exhibit similar behavior.

The sharp features in the IVC become smeared on approaching T_c . They are hysteretic, with the transition from Josephson to normal state always occurring at higher current, as expected for underdamped Josephson junctions in the resistively and capacitively shunted junction (RCSJ) model.¹⁹ The switching current is sensitive to magnetic field, as illustrated by the Fraunhofer pattern in the lower inset of Fig. 1(a). To obtain the value of I_c in zero field, we apply a compensating field tuned to maximize its value. Another type of switching induced by sweeping V_g is illustrated in Fig. 1(b). As before, sharp switching is seen between the Josephson and the normal current states, this time as a function of V_g . Here, too, we observe hysteresis. In the RCSJ model, both cases correspond to runaway of the “phase particle” moving in a tilted washboard potential $U(\varphi) = -E_J[\cos(\varphi) + (I/I_c)\varphi]$ with average slope $\sim I/I_c$, where φ is the phase difference between the two superconducting banks, and $E_J = \Phi_0 I_c / 2\pi$ is the Josephson energy. The slope is controlled by I or by I_c for the current or gate swept measurements, respectively. Figure 1(c) illustrates the variation of R_n , the resistance in the normal state, as V_g is swept through the Dirac point (DP) causing the charge carriers to change from holes (negative V_g) to electrons (positive V_g). The low temperature normal state was accessed by quenching the superconductivity in the leads with a small magnetic field. As

discussed below and illustrated in Fig. 3(a), the switching currents measured here are significantly lower than theoretical predictions for ballistic junctions.

For a homogeneous charge distribution, the mean free path, l , can be estimated from the measured normal state conductivity, σ , using $l = \sigma h / 2e^2 k_F$ and $k_F = \sqrt{\epsilon \epsilon_0 V_g \pi} / ed$. Here, $d=300$ nm is the thickness of the SiO_2 layer and $\epsilon \sim 4$ its dielectric constant. Away from the neutrality point (NP), $|V_g| > 10$ V, where the random potential due to substrate and other inhomogeneities is well screened,^{20,21} k_F and l can be estimated from V_g . Here, l weakly depends on gate voltage suggesting comparable contributions from short range and long range scatterers.^{22–24} We find that its value for all SGS samples on SiO_2 substrates is much shorter than the lead distance, $l \sim 25 \text{ nm} \ll L$, indicating that the SGS junctions are diffusive. Interestingly, this result holds for all SGS samples supported on SiO_2 and with Al/Ti leads—our own as well as those reported by other groups.^{5,6}

It was recently shown that close to the NP, the charge distribution breaks up into electron-hole puddles.^{20,21} Here, the carrier density roughly remains constant and the MFP can no longer be estimated from the V_g dependence of the conductivity. We found that the empirical relation $\sigma h / 2e^2 k_F \sim V_g^{-1/2}$, obtained by assuming constant carrier density, is useful for identifying the puddle regime. Its onset, indicated by the arrow in the inset of Fig. 1(c), is sharp and easy to recognize. Since the formation of the puddles cannot increase the MFP, the data for the entire range of gate voltages

were analyzed under the diffusive assumption. Estimating the superconducting coherence length in the diffusive limit: $\xi \sim \sqrt{\hbar D / \Delta} \sim 250 \text{ nm} \sim L$, where $D = \nu_F l / 2$ is the diffusion coefficient, we find that our SGS devices are at the crossover between long and short diffusive Josephson junctions. In Fig. 1(d), we compare the gate dependence of I_c (green curve) to calculated values for ballistic SGS junctions⁹ (solid black curve). We note that the discrepancy between the measured and calculated values rapidly increases with gate voltage, until at the highest gate voltages it exceeds 1 order of magnitude. Clearly, the gate dependence of I_c in these SGS junctions cannot be accounted for in the picture of ballistic transport.

MULTIPLE ANDREEV REFLECTIONS

It is well known that the value of I_c is sensitive to fluctuations introduced by the environment, making it difficult to compare with theoretical predictions. By contrast, the structure that appears in the IVC due to MAR is robust and will be used here to compare to theoretical predictions, which are distinctly different for ballistic and diffusive junctions. In the diffusive junction model, the MAR features are independent of carrier density but their shape is quite sensitive to the ratio L/ξ . On the other hand, in the ballistic SGS junction model,¹⁵ the MAR features are independent of L/ξ but are quite sensitive to carrier density with the normalized conductivity at the first MAR maximum sharply dropping from 4.5 at the DP to ~ 1.5 away from it. The data in Fig. 2(a) show the pronounced MAR features that develop in the bias voltage dependence of the differential resistance below T_c . These features consist of a series of sharp resistance minima appearing at subgap voltages $2\Delta/pe$, where p is an integer and Δ is the superconducting gap of the electrodes. The first four MAR minima are indicated by dotted lines. For all our samples, the first four to six minima are easily identified, indicating high transparency of the SG interfaces. The subgap features, whose temperature dependence tracks $\Delta(T)$, are essentially independent of temperature below 500 mK. In Fig. 2(b), we plot the bias dependence of the normalized conductivity for three representative values of V_g (these data were taken on another sample S022207 with $L=220 \text{ nm}$, $W=2.8 \mu\text{m}$, and $R_{n,\text{max}}=465 \Omega$). We find that the curves overlap for all gate voltages except for a slightly different shape of the first MAR peak at the DP which is attributed to a reduced mean free path there.²⁵ The shape of MAR features in diffusive junctions is quite sensitive to the ratio L/ξ . Comparing the shape of the measured MAR features with theoretical predictions,²⁵ we find that they best fit diffusive junctions with $L/\xi \sim 1-2$. This yields a coherence length $\xi = 150-300 \text{ nm}$, which corresponds to $l \sim 2\Delta\xi^2/\hbar v_F \sim 10-30 \text{ nm}$, in agreement with the values obtained from the normal resistance of the device. For a more quantitative analysis, we measured normalized differential conductance at the first subgap peak ($p=1$) and plotted it against the ratio L/ξ (with ξ obtained from gate dependence of resistivity in the normal state), as illustrated in the inset of Fig. 2(b). The data points from our samples, as well as from the single other published data⁵ on MAR in SGS samples, nicely fall

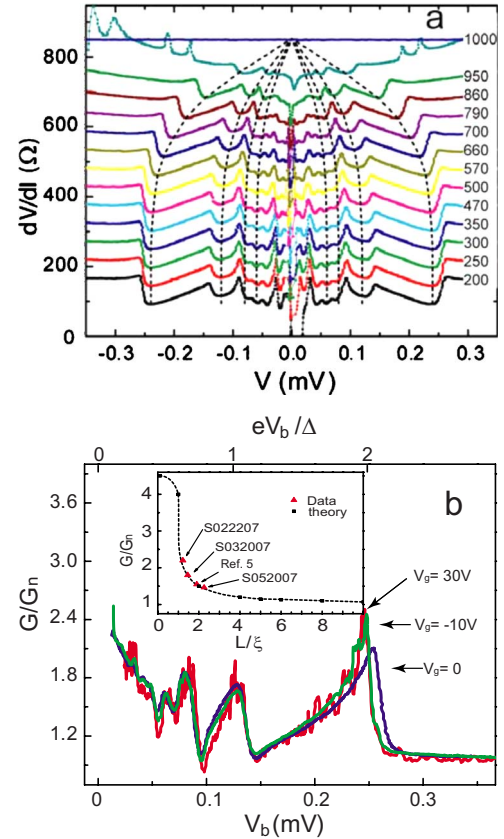


FIG. 2. (Color online) Multiple Andreev reflections. (a) Temperature dependence of the MAR. Curves, taken for different temperatures, are vertically shifted for clarity. The labels show temperatures in units of mK. Dotted lines indicate the first four subgap oscillations. The extra peaks at high bias (seen in the curve just below T_c) signal the superconducting to normal transition in the leads. (b) Comparison of normalized subgap features at different doping levels for sample S022207. Inset: normalized differential conductance as a function of L/ξ . Black squares, theoretical values for diffusive junctions from Ref. 25. Triangles, measured values. A similar estimate for the data in Ref. 6 was not possible because the Andreev reflections were absent.

onto the theoretical curve derived for junctions in the diffusive regime.²⁵

COMPARISON WITH DIFFUSIVE JUNCTION MODEL

We next compare the measured values of I_c and $I_c R_n$ to calculated values obtained for diffusive SNS junctions. The reduction of these quantities due to scattering in the diffusive regime is captured by the Likharev model^{26,27} which we adopt here for the data analysis. The model treats the junction as a 1- d weak link with vanishing gap in the channel material. By using the MFP obtained from the measured V_g dependence of R_n , as an input parameter,²⁸ we numerically solved Usadel's equations²⁹ to obtain an expression for the temperature dependence of $V_c^{\text{cal}} \equiv I_c^{\text{cal}} R_n$ and I_c^{cal} as a function of gate voltage (*cal* refers to calculated values). As illustrated in Fig. 3(a), the overall temperature dependence of I_c^{cal} qualitatively agrees with the measurement, but its magnitude is

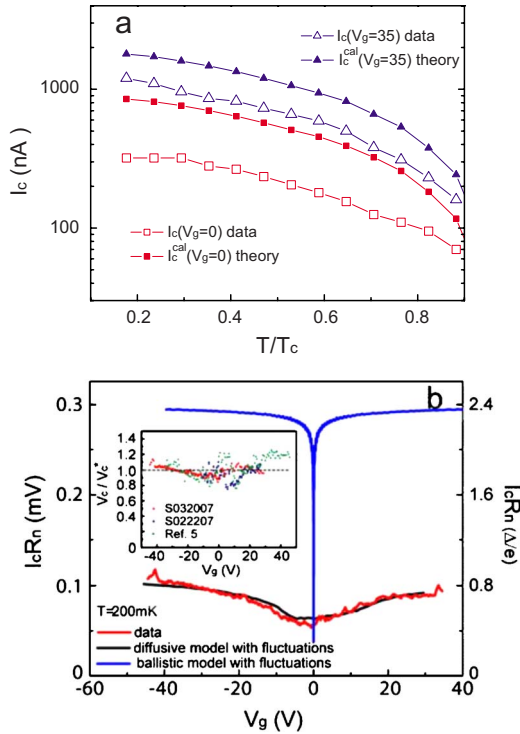


FIG. 3. (Color online) Temperature and gate dependence of the Josephson effect. (a) Comparison of the measured temperature dependence of the switching current, I_c , with calculated values for ballistic SGS junctions, I_c^{cal} . (b) Comparison of measured gate dependence of $V_c = I_c R_n$ —red curve (gray)—with calculated values from Likharev’s model including corrections for premature switching $V_c^* = I_c^* R_n$ (black curve). The blue curve (dark gray) corresponds to the ballistic model. Inset: ratio of experimental and theoretical values V_c/V_c^* , for two of our samples: S032007, S022207, and for data obtained from Ref. 5. The solid line is a guide to the eye.

consistently larger (~ 1.5 and 2.5 times larger near the NP and at $V_g = 40$ V, respectively). This discrepancy is attributed to “premature” switching induced by fluctuations due to the thermal and electromagnetic noise.^{30,31} The mean reduction in critical current can be estimated in the limit $E_J \gg E_{fl}$, as $\langle \Delta I_c \rangle \sim I_c \left[\frac{E_{fl}}{2E_J} \ln \left(\frac{\omega_p \Delta t}{2\pi} \right) \right]^{2/3}$. Here, $E_J = \hbar I_c / 2e$ is the Josephson energy, E_{fl} is a characteristic fluctuation energy, $\Delta t \sim 10^2 - 10^3$ s the measurement time, $\omega_p = \sqrt{2eI_c / \hbar C} \sim 10^{11}$ s $^{-1}$ is the plasma frequency of the junction, and $C \sim 2 \times 10^{-13}$ F is the effective capacitance estimated from the RCSJ model.¹⁹ Assuming that the thermal and radiation noise are additive, we write $E_{fl} \sim k_B(T + T_{EM})$, with T_{EM} an effective temperature increase due to the radiation energy. In Fig. 3(b), we compare gate voltage dependence of the measured $V_c \equiv I_c(V_g)R_n(V_g)$ (red curve) with the calculated values corrected for fluctuations: $V_c^* = I_c^*(V_g)R_n(V_g)$ (black curve), where $I_c^* = I_c^{cal} - \langle \Delta I_c \rangle$ is the critical current corrected for fluctuations. We now find that the measured and calculated values overlap over the entire range of V_g . The fluctuation correction was obtained by assuming a single value for $T_{EM} \sim 300$ mK, which is consistent with our experimental setup and level of shielding. By contrast, in order to match ballistic junction predictions, one would have to assume

noise temperatures that are unrealistically high, which moreover would have to depend on gate voltage. We wish to stress that T_{EM} is a parameter introduced to quantifying the effect of noise on the superconducting phase slippage and it does not necessarily affect the electronic temperature. This can be seen in Fig. 3(a), where I_c continues to monotonically grow as the temperature decreases well below $T = T_{EM}$.

CONCLUSION

We have shown that the characteristic transport features, expected to arise due to ballistic transport and to the relativistic nature of charge carriers, are conspicuously absent in the SGS junctions. In particular, we do not observe the gate dependence of the MAR and of the I_c predicted by the ballistic theory. The absence of these features is due to the two primary limiting factors: short mean free paths and the smearing of the Dirac point by electron-hole puddles. It is possible that neither limitation is intrinsic to SGS junction. Mean free paths of 100 nm are routinely achieved in our samples as well as in those reported by other groups, for large lead separations, 500 nm the highest reported so far, so it would seem that the MFP is reduced by the deposition of the Al/Ti leads. Optimizing the lead material and fabrication technique to reduce its invasiveness could help achieve ballistic transport. The electron-hole puddles, which broaden the DP, are the result of substrate associated trapped charges and the poor screening afforded by the low carrier density and the low dimensionality. For samples deposited on SiO₂ substrates, the puddles were found^{20,21} to smear the DP by more than 2 V in terms of gate voltage, corresponding to a Fermi level broadening of $\delta E_F = \hbar v_F \sqrt{\epsilon \epsilon_0 \delta V_g \pi / ed} \sim 45$ meV $\gg \Delta = 0.12$ meV. This broadening violates one of the necessary conditions for observing effects due to the relativistic nature of the charge carriers, such as SAR or the predicted gate dependence of the MAR and I_c . If these effects are to be observed, the spread of the DP cannot exceed the energy scale of the gap.¹⁴ This would require charge uniformity corresponding to a gate control of $V_g < 0.1$ mV (for Al leads) and $V_g < 0.1$ V (for HTC superconductors), conditions that are not compatible with present fabrication techniques.

The work described here demonstrates that, contrary to expectations, the transport in SGS junctions on SiO₂ substrates is diffusive rather than ballistic, resembling the properties of junctions with metallic weak links. This is, in fact, the case for all SGS junctions fabricated to date, our own as well as those reported by other groups. The diffusive transport in these junctions is a result of the short mean free path and smearing of the DP caused by scattering from substrate induced charge inhomogeneities. We have now directly proved this fact in a new series of experiments by showing that removal of the substrate results in a tenfold increase in the mean free path.³² Similar results were also reported by another group.³³ A surprising and important aspect of SGS physics revealed by this work is that they display sharp and well-defined sequences of MAR, demonstrating that even when supported on SiO₂ these devices have almost ideal interfaces. The high quality of the interfaces together with the

gate tunable and bipolar carrier density makes the SGS devices ideal candidates for superconducting circuit applications. At the same time, they provide a powerful and flexible probe for exploring the phase diagram of the Josephson effect with one single device.¹⁰ Such degree of versatility cannot be attained with any other known junction materials: metallic junctions are not tunable and in semiconductor junctions, it is difficult to produce transparent interfaces.

ACKNOWLEDGMENTS

We thank J. Wei, J. Sanchez, G. Li, Z. Chen, and J. Appenzeller for discussions, S. W. Cheong and M. Gershenson for use of AFM and e-beam, and V. Kiryukhin and A. F. Hebard for HOPG crystals. This work was supported by DOE Contract No. DE-FG02-99ER45742, NSF Grant No. DMR-0456473, and ICAM.

-
- ¹K. S. Novoselov, A. K. Geim, S. V. Morozov, D. Jiang, Y. Zhang, S. V. Dubonos, I. V. Grigorieva, and A. A. Firsov, *Science* **306**, 666 (2004).
- ²K. S. Novoselov, A. K. Geim, S. V. Morozov, D. Jiang, M. I. Katsnelson, I. V. Grigorieva, S. V. Dubonos, and A. A. Firsov, *Nature (London)* **438**, 197 (2005).
- ³Y. Zhang, Y.-W. Tan, H. L. Stormer, and P. Kim, *Nature (London)* **438**, 201 (2005).
- ⁴A. H. Castro Neto, F. Guinea, N. M. R. Peres, K. S. Novoselov, and A. K. Geim, arXiv:0709.1163, *Rev. Mod. Phys.* (to be published).
- ⁵H. B. Heersche, P. Jarillo-Herrero, J. B. Oostinga, L. M. K. Vandersypen, and A. F. Morpurgo, *Nature (London)* **446**, 56 (2007).
- ⁶F. Miao, S. Wijeratne, Y. Zhang, U. C. Coskun, W. Bao, and C. N. Lau, *Science* **317**, 1530 (2007).
- ⁷Y.-J. Doh, J. A. van Dam, A. L. Roest, E. P. A. M. Bakkers, L. P. Kouwenhoven, and S. De Franceschi, *Science* **309**, 272 (2005).
- ⁸H. Takayanagi and T. Kawakami, *Phys. Rev. Lett.* **54**, 2449 (1985).
- ⁹M. Titov and C. W. J. Beenakker, *Phys. Rev. B* **74**, 041401(R) (2006).
- ¹⁰J. M. Kivioja, T. E. Nieminen, J. Claudon, O. Buisson, F. W. J. Hekking, and J. P. Pekola, *Phys. Rev. Lett.* **94**, 247002 (2005).
- ¹¹A. F. Andreev, *Sov. Phys. JETP* **19**, 1228 (1964).
- ¹²I. O. Kulik, *Sov. Phys. JETP* **30**, 944 (1970).
- ¹³G. E. Blonder, M. Tinkham, and T. M. Klapwijk, *Phys. Rev. B* **25**, 4515 (1982).
- ¹⁴C. W. J. Beenakker, *Phys. Rev. Lett.* **97**, 067007 (2006).
- ¹⁵J. C. Cuevas and A. L. Yeyati, *Phys. Rev. B* **74**, 180501(R) (2006).
- ¹⁶M. Maiti and K. Sengupta, *Phys. Rev. B* **76**, 054513 (2007).
- ¹⁷M. I. Katsnelson and K. S. Novoselov, *Solid State Commun.* **143**, 3 (2007).
- ¹⁸T. Ando, *J. Phys. Soc. Jpn.* **75**, 074716 (2006).
- ¹⁹W. C. Stewart, *Appl. Phys. Lett.* **12**, 277 (1968).
- ²⁰J. Martin, N. Akerman, G. Ulbricht, T. Lohmann, J. H. Smet, K. von Klitzing, and A. Yacoby, *Nat. Phys.* **4**, 144 (2008).
- ²¹S. Cho and M. S. Fuhrer, *Phys. Rev. B* **77**, 081402(R) (2008).
- ²²K. Nomura and A. H. MacDonald, *Phys. Rev. Lett.* **98**, 076602 (2007).
- ²³E. H. Hwang, S. Adam, and S. Das Sarma, *Phys. Rev. Lett.* **98**, 186806 (2007).
- ²⁴M. I. Katsnelson and A. K. Geim, *Philos. Trans. R. Soc. London, Ser. A* **366**, 195 (2008).
- ²⁵J. C. Cuevas, J. Hammer, J. Kopu, J. K. Viljas, and M. Eschrig, *Phys. Rev. B* **73**, 184505 (2006).
- ²⁶K. K. Likhorev, *Sov. Tech. Phys. Lett.* **2**, 12 (1976).
- ²⁷K. K. Likhorev, *Rev. Mod. Phys.* **51**, 101 (1979).
- ²⁸Estimates of the mean free paths near the DP were obtained by extrapolation of the values from higher gate voltages to $V_g=0$ as illustrated by the solid (red) dot in the inset of Fig. 1(c).
- ²⁹K. D. Usadel, *Phys. Rev. Lett.* **25**, 507 (1970).
- ³⁰T. A. Fulton and L. N. Dunkleberger, *Phys. Rev. B* **9**, 4760 (1974).
- ³¹M. Tinkham, *Introduction to Superconductivity* (McGraw-Hill, New York, 1996).
- ³²X. Du, I. Skachko, A. Barker, and E. Y. Andrei, arXiv:0802.2933, *Nat. Nanotechnol.* (to be published).
- ³³K. I. Bolotin, K. J. Sikes, Z. Jiang, G. Fudenberg, J. Hone, P. Kim, and H. L. Stormer, arXiv:0802.2389 (unpublished).